Available online at www.sciencedirect.com

ScienceDirect

Procedia IUTAM 14 (2015) 274 – 281

Procedia IUTAM

www.elsevier.com/locate/procedia

IUTAM_ABCM Symposium on Laminar Turbulent Transition

Bypass transition in three-dimensional time-dependent boundary layers

M. J. Philipp Hack[a], Tamer A. Zaki[a,b,*]

[a]*Department of Mechanical Engineering, Imperial College, London SW7 2AZ, United Kingdom*
[b]*Department of Mechanical Engineering, Johns Hopkins University, Baltimore, MD 21218, United States*

Abstract

The influence of spanwise wall oscillation on transition in boundary layers exposed to free-stream turbulence is examined. Results from direct numerical simulations show that for moderate amplitudes of the wall motion, transition to turbulence can be considerably delayed. On the other hand, high-amplitude forcing leads to breakdown to turbulence upstream of the unforced reference flow configuration. Flow visualizations and statistical results show that the stabilization of the flow at the optimal forcing parameters is the result of a substantial weakening of the low-frequency boundary layer streaks. On the other hand, the early breakdown at high forcing amplitudes is associated with the amplification of new high-frequency instabilities in the pre-transitional flow.

Selection and peer-review under responsibility of ABCM (Brazilian Society of Mechanical Sciences and Engineering)
Keywords: Bypass transition;

1. Introduction

Exposure of a laminar boundary layer to moderate levels of free-stream disturbances leads to a rapid breakdown to turbulence — a process known as bypass transition. Earlier studies have focused on explaining the underlying mechanism of bypass transition, and more recently on its control. The present study examines the influence of spanwise harmonic wall motion on the transition process.

Classical stability theory attributes the earlier stages of transition to turbulence in boundary layers to the exponential growth of infinitesimal disturbances, known as Tollmien-Schlichting (TS) waves, once a critical Reynolds number is exceeded[1]. This natural transition process is bypassed in the presence of moderate levels of free-stream disturbances, and a more rapid breakdown mechanism takes effect. Experimental studies established that the bypass process becomes dominant for initial disturbance amplitudes in excess of approximately 1%[2]. Reviews of bypass transition are provided for example by Durbin and Wu[3] and Zaki[4].

Linear analyses[5,6,7] showed that the mean shear acts as a low-pass filter which prevents the high-frequency component of the free-stream spectrum from entering the boundary layer. Low-frequency disturbances are unaffected by this filtering effect of the shear and retain their amplitude inside the boundary layer where they cause the formation

* Corresponding author. Tel.: +1-410-516-6599.
E-mail address: t.zaki@jhu.edu

Selection and peer-review under responsibility of ABCM (Brazilian Society of Mechanical Sciences and Engineering)
doi:10.1016/j.piutam.2015.03.050

of streaks[8]. The generation of these streamwise elongated perturbations can be explained in terms of the vertical displacement of the mean momentum of the boundary layer, commonly referred to as "lift-up"[9,10]. The highly energetic streaks promote the growth of high-frequency secondary instabilities[11,12,13]. In zero-pressure-gradient boundary layers, breakdown to turbulence is predominantly initiated via so-called outer modes, which are situated on top of low-speed streaks that are lifted to the boundary-layer edge. Inner instabilities are also possible[12]. Although less aggressive in zero pressure gradient, inner instability can become dominant in adverse pressure gradients[14,13]. The streak instabilities induce the local formation of turbulent spots, which eventually merge to form a contiguous region of turbulent flow.

The significant increase in skin friction in the fully-turbulent flow regime motivates two approaches to drag reduction: the first attempts to alter the turbulent state and the second aims to avoid it altogether by stabilizing the pre-transitional flow. A wealth of studies have pursued the first option, and established that spanwise wall oscillation can substantially reduce skin friction in fully-turbulent flows. That body of research was motivated by investigations of swept-wing boundary layers, which showed that the rapid change of the flow direction induced by the transverse pressure gradient leads to a noticeable reduction of the local skin friction[15]. Building on these results, Driver and Hebbar[16] and Spalart[17] demonstrated that turbulent streaks are absent in flows with continuously changing mean direction. Jung et al.[18] conducted parameter studies of spanwise wall forcing in turbulent channel flow using DNS. A reduction of the mean wall-shear-stress was observed for oscillation periods $25 < T^+ < 200$, where $T^+ = Tu_\tau^2/\nu$ and u_τ is the friction velocity. Energetic considerations showed that when the power input into the wall motion is taken into account, forcing with optimal parameters can yield net energetic savings of about 7%[19].

In the present study, attention is focused on the transition regime. Direct numerical simulations are performed in order to examine the influence of spanwise wall oscillation on bypass transition in boundary layers.

2. Simulation setup

The incompressible Navier-Stokes equations are solved using a fractional step approach[20] and a finite-volume discretization[21]. The convective terms are advanced in time using an Adams-Bashforth scheme, and the diffusion terms are treated implicitly with a Crank-Nicolson scheme. The Poisson equation for the pressure is solved by applying Fourier and cosine transforms along the spanwise and streamwise directions, and direct inversion is employed in the wall-normal coordinate.

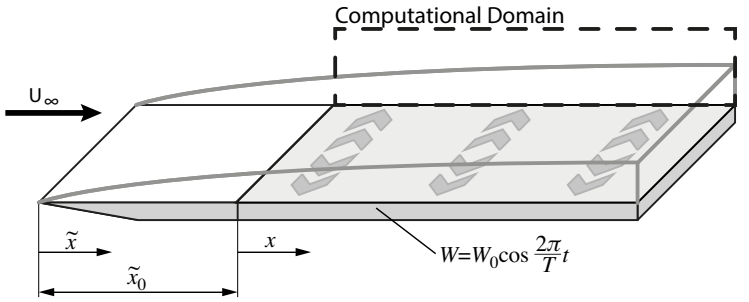

Fig. 1. Schematic of the problem setup and the computational domain.

A graphical representation of the simulation setup is provided in Fig. 1. The computational domain starts at distance $\tilde{x}_0$ to the leading edge of the flat plate, at the origin of the coordinate $x \equiv \tilde{x} - \tilde{x}_0$. Spanwise wall oscillation is applied over the full extent of the computational domain by imposing the wall boundary condition,

$$W(y = 0, t) = W_0 \cos\left(\frac{2\pi}{T} t\right). \tag{1}$$

All length scales are normalized by the inlet 99% boundary-layer thickness, δ_0, and velocities are normalized by the free-stream value, U_∞. The inlet Reynolds number based on δ_0 is $\mathrm{Re}_{\delta_0} = 800$. The length, width and height of the

computational domain are 1200, 30 and 40, respectively, and the number of grid points in these dimensions are 4096, 192 and 192.

In order to account for the periodic flow component introduced by the wall forcing, a triple decomposition is applied to the flow variables,

$$a = \overbrace{\bar{a} + \underbrace{\tilde{a}_\varphi}_{a''}}^{\langle a \rangle_\varphi} + a', \tag{2}$$

where $\bar{a}$ denotes the spanwise and time-average, $\tilde{a}_\varphi$ is the periodic component and a' is the stochastic fluctuation. The quantity $\langle a \rangle_\varphi$ is the average at a particular phase, and comprises the time-averaged mean and the periodic component. The total fluctuation a'' is the sum of the periodic component and the stochastic fluctuation.

Bypass transition is induced by superimposing a moderate level of isotropic free-stream turbulence ($Tu_{\mathrm{FS}} = 3\%$) onto the Blasius profile at the inlet of the computational domain. The perturbation field is synthesized in terms of a weighted superposition of continuous Orr-Sommerfeld and Squire modes[22]. This approach faithfully reproduced the experimental data of bypass transition of Roach and Brierley[23], and was later adopted in a number of studies of transitional flows[24,25,14]. The downstream evolution of the root-mean-square (rms) of the cartesian velocity components in the free stream is presented in Fig. 2. An isotropic decay of the external perturbation field is observed, which follows the power law $Tu_{\mathrm{FS}} \sim \tilde{x}^{-0.69}$.

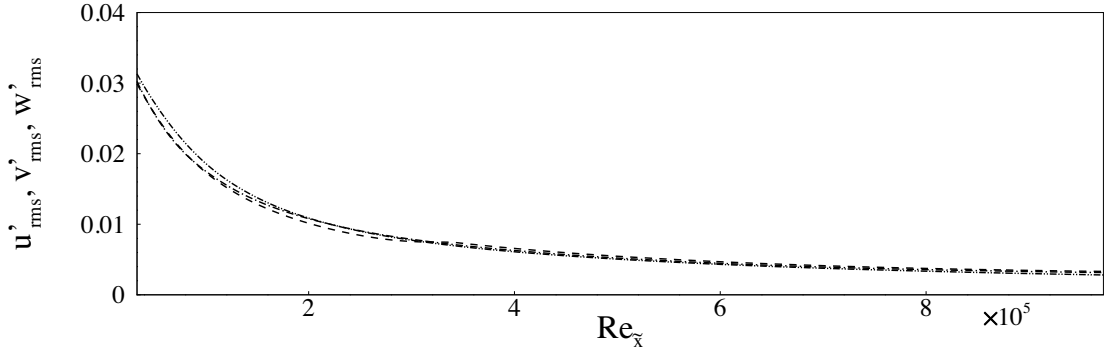

Fig. 2. Free-stream decay of turbulence: (a) Rms of the velocity fluctuations u' (dashed), v' (dash-dotted), w' (dash-dot-dotted) as a function of the Reynolds number $Re_{\tilde{x}}$.

3. Results

Direct simulations were performed for a wide range of wall-oscillation parameters. Here, the focus is placed on the influence of the amplitude of the wall motion when the period of the forcing is kept constant at $T = 200$. The skin friction coefficient,

$$C_f = \frac{\mu \frac{\partial U}{\partial y}|_{y=0}}{\frac{1}{2}\rho U_\infty^2}, \tag{3}$$

is shown in Fig. 3*a* as a function of the Reynolds number. Forcing with $W_0 = 0.10$ leads to a moderate delay of the transition process. A more pronounced stabilization of the laminar regime is observed at $W_0 = 0.25$. However, when the forcing amplitude is increased to $W_0 = 0.40$, transition to turbulence occurs significantly earlier than in the unforced reference simulation.

In order to establish whether transition delay at moderate forcing amplitudes translates into a net energetic advantage, the power input into the wall motion, $\overline{P}_{\mathrm{forcing}}$, has to be taken into account. The reduction in propulsion power

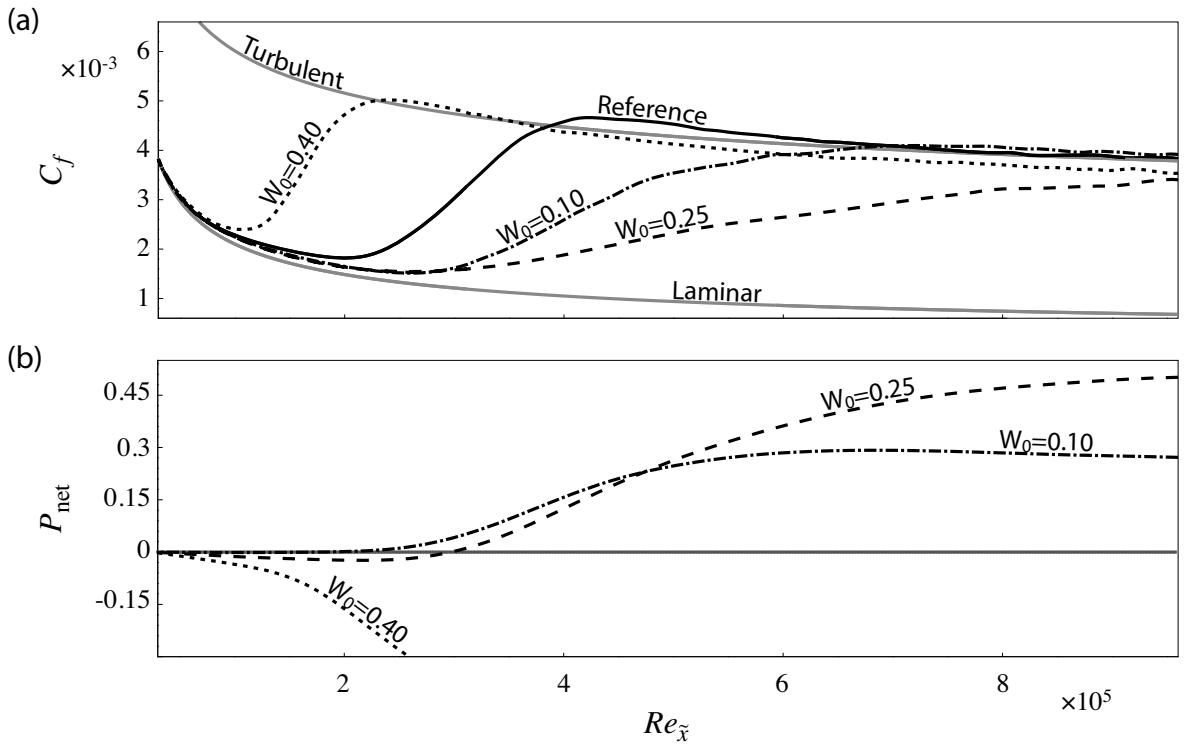

Fig. 3. Skin friction coefficient and net energetic savings as a function of the Reynolds number. Reference case (solid), forcing with $W_0 = 0.10$ (dash-dotted), forcing with $W_0 = 0.25$ (dashed) and forcing with $W_0 = 0.40$ (dotted).

compared to an unforced reference flow is $\Delta\overline{P}_{\text{prop}} \equiv \overline{P}_{\text{prop,ref}} - \overline{P}_{\text{prop,forced}}$, and the net energetic savings are hence defined as $\overline{P}_{\text{net}} \equiv \Delta\overline{P}_{\text{prop}} - \overline{P}_{\text{forcing}}$. Results for the net savings are presented in Fig. 3*b*. Forcing with amplitudes $W_0 = 0.10$ and 0.25 indeed translates into a net energetic advantage. In the optimal case, $W_0 = 0.25$, the reduction in propulsion power exceeds the input into the wall motion by a factor of more than four. The net savings thus significantly exceed the energetic advantage reported in the literature on fully-turbulent flows [19,26].

3.1. Transition delay

A key feature of the influence of wall forcing on the transitional boundary layer is captured in the visualizations in Fig. 4. The first frame shows a top view of the reference case in the absence of any wall motion. Isosurfaces of the streamwise velocity fluctuation indicate highly energetic boundary layer streaks, some of which show the streamwise undulation characteristic of the amplification of high-frequency secondary instabilities. A turbulent spot is observed around $x = 240$, and the flow is fully turbulent downstream of $x \approx 400$. The second frame depicts the case with wall oscillation, $W_0 = 0.25$. Compared to the reference case, streak amplitudes are markedly reduced, and there are no visible indications of secondary instabilities. The flow remains laminar over the entire extent of the depicted region. Studies of time series show that this stabilization of the boundary layer streaks is a persistent phenomenon that is not limited to particular phases of the wall oscillation.

The weakening of streaks which is observed in the instantaneous realization (Fig. 4) can be quantified using statistics of the streamwise velocity fluctuations. Fig. 5 provides the maximum level of the rms of u' inside the boundary layer as a function of the Reynolds number. In the reference case (solid line), the streaks begin to saturate at $Re_{\tilde{x}} \approx 2 \times 10^5$, and a maximum intensity of approximately 17% is reached at $Re_{\tilde{x}} \approx 3.3 \times 10^5$. This location correlates with the local maximum of the skin friction curve (Fig. 3*a*), which is commonly associated with the completion of

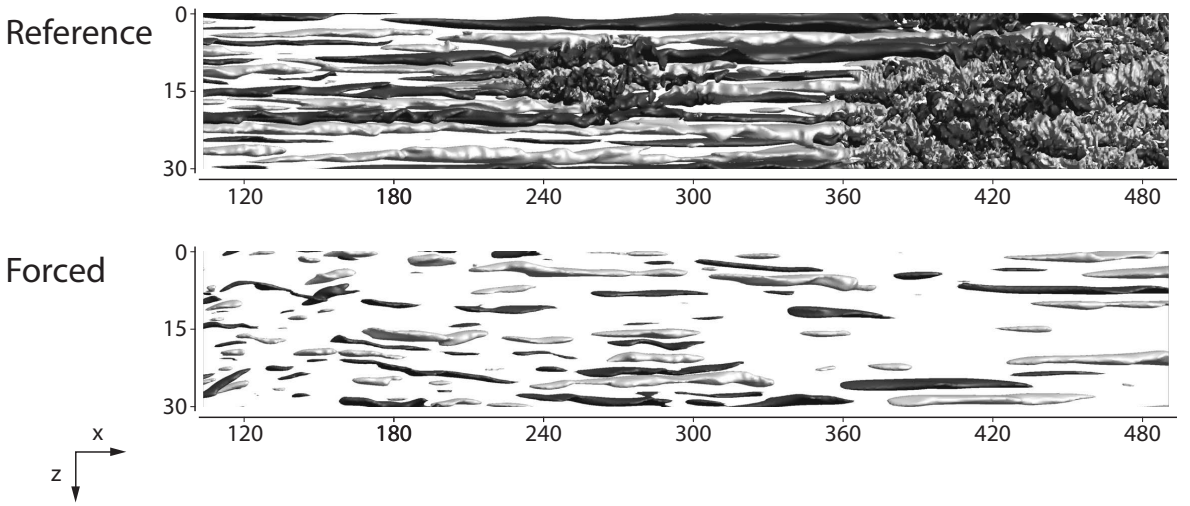

Fig. 4. Top views with isosurfaces of high-speed (white, $u' = 0.085$) and low-speed (black, $u' = -0.085$) streaks. Unforced reference case and wall oscillation with $T = 200$, $W_0 = 0.25$.

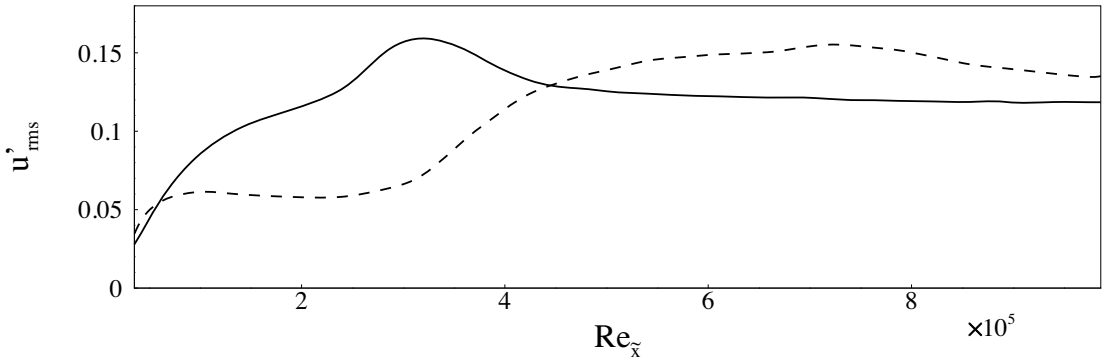

Fig. 5. Maximum rms of the streamwise velocity fluctuation over all wall distances as a function of the Reynolds number. Reference simulation (solid) and forcing with $W_0 = 0.25$ (dashed).

transition to turbulence. In the presence of the wall oscillation, the growth of streaks is noticeably weakened, and the streamwise fluctuations initially plateau at 6%. The peak value of 17% matches the references case, although it is reached significantly farther downstream.

3.2. Promoting transition

At high wall-oscillation amplitude, $W_0 = 0.40$, transition takes place early upstream. A time series of top views of the flow field for this case is provided in Fig. 6. It is initiated by short-scale instability, significantly shorter than the streaks in the unforced reference simulation, cf. Fig. 4. The frames capture the evolution of the instability and show the formation of a turbulent spot. While the intensity of the perturbations in the laminar portion of the boundary layer clearly increases between $\varphi = 0.125$ and $\varphi = 0.250$, it has decayed again at $\varphi = 0.500$. This observation indicates a strong phase dependence of the underlying instability amplification mechanism.

Spectral analysis confirms the qualitative change of the fluctuation field in the pre-transitional boundary layer in response to the high-amplitude forcing. The Fourier coefficients of the wall-normal fluctuations were evaluated in the

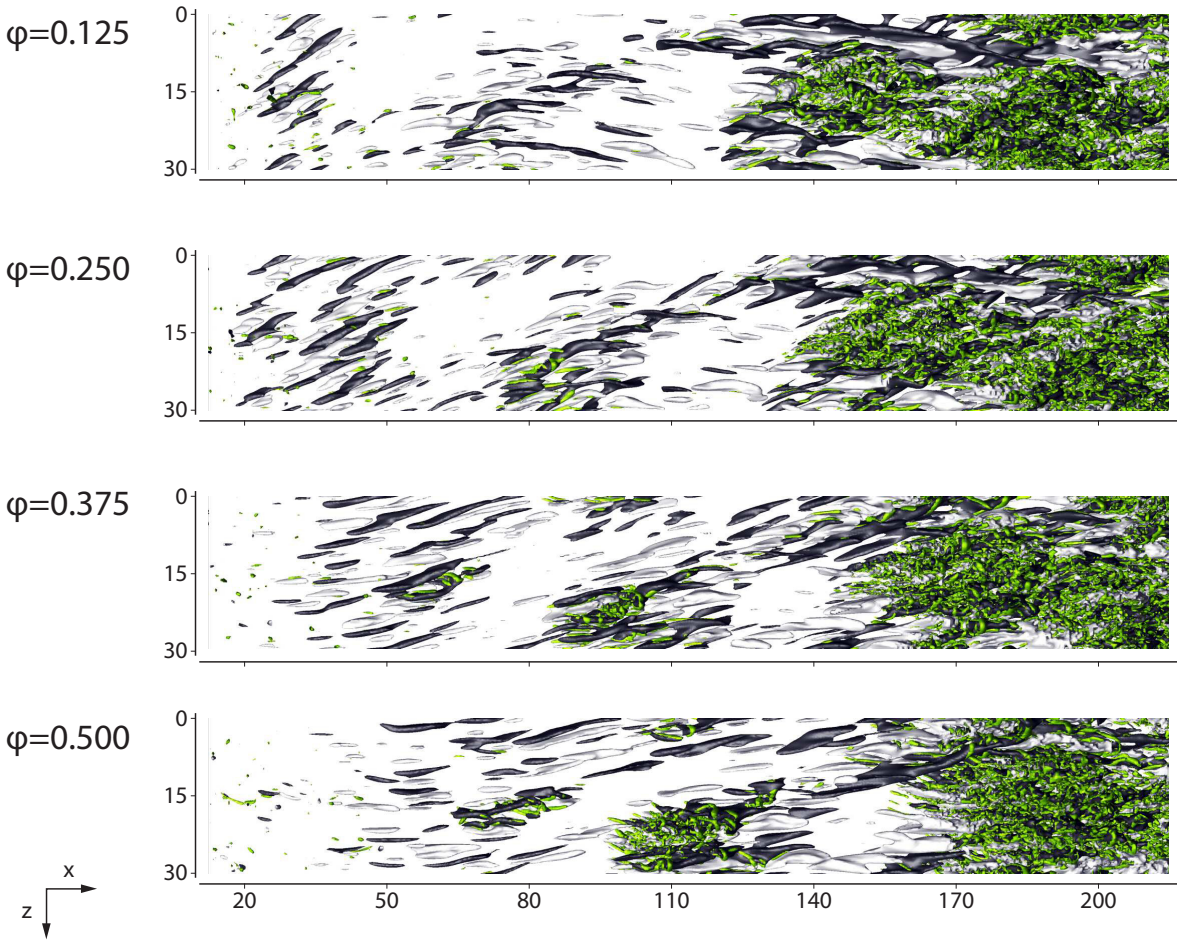

Fig. 6. Top views with isosurfaces of positive (white, $u' = 0.085$) and negative (black, $u' = -0.085$) velocity perturbations as well as the Q criterion (green/gray) for identifying vortical structures at four different phases. High-amplitude wall forcing with $T = 200$, $W_0 = 0.40$.

region $75 < x < 130$,

$$\hat{v}(\alpha,\beta) = \frac{1}{N}\sum_{n=1}^{N}\int_{-\infty}^{\infty}\int_{-\infty}^{\infty} v' \exp\left(-2\pi \mathrm{i}\left(\alpha x + \beta z\right)\right)\, \mathrm{d}x\, \mathrm{d}z, \tag{4}$$

where $N = 4,000$ is the number of samples. A Hann window is used for the streamwise dimension. The magnitudes of the Fourier coefficients are presented in Fig. 7*a* for the unforced reference case as a function of the streamwise and spanwise wave numbers. In the absence of the wall forcing, the maximum intensity is recorded at $\alpha \approx 0.1$, $\beta \approx 2.5$, which reflects the very low frequency of the fluctuation field inside the boundary layer. The presence of the high-amplitude wall oscillation fundamentally changes the spectral composition of the perturbations inside the boundary layer (see Fig. 7*b*). The fluctuation field becomes dominated by short-scale disturbances with streamwise wave numbers in excess of 0.5, consistent with the prevalence of high-frequency perturbations in Fig. 6.

The early breakdown at high forcing amplitudes proceeds without the mediation of Klebanoff streaks, and is therefore entirely different from conventional bypass transition. A potential cause of the observed behavior is the occurrence of a powerful modal growth mechanism in the three-dimensional boundary layer that becomes active beyond a certain amplitude of the wall oscillation, akin to cross-flow instability.

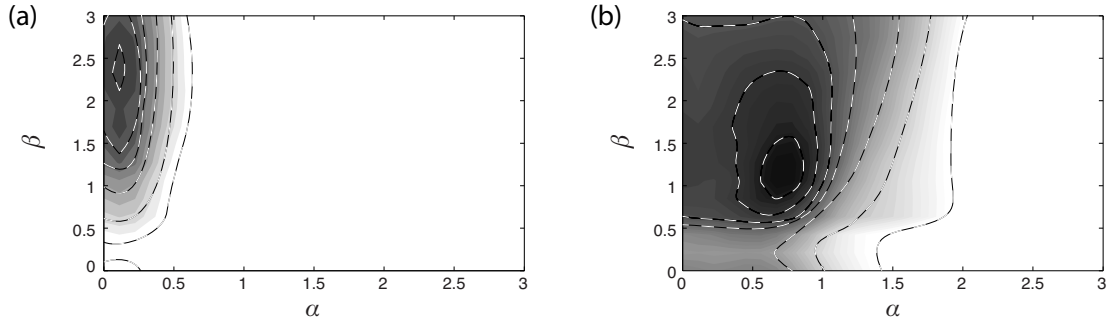

Fig. 7. Contours of the magnitude of the Fourier coefficients of the wall-normal fluctuation component, $|\hat{v}|$, as a function of the streamwise and spanwise wavenumber fluctuation wavenumber. (a) Reference case. (b) Wall oscillation with $W_0 = 0.40$.

4. Conclusions

The effect of spanwise wall oscillation on bypass transition in boundary layers beneath free-stream turbulence was investigated by means of direct numerical simulations. At constant frequency of the wall motion, changes in the oscillation amplitude can dramatically influence the transition mechanism and the location of breakdown to turbulence. Wall oscillation with moderate amplitudes considerably weakens the boundary layer streaks and, as a result, the subsequent stages of the bypass process. The outcome is a significant downstream shift of transition to turbulence. Energetic considerations showed that the associated reduction of viscous friction drag clearly exceeds the power input into the wall motion, and a considerable net energetic advantage is achieved.

Forcing with high amplitudes initiated an early breakdown upstream of the unforced reference simulation. Spectral analyses confirmed empirical observations from instantaneous flow fields: A new transition mechanism becomes active. The high-amplitude forcing promotes the growth of short-scale disturbances that induce early breakdown to turbulence. The amplification of these perturbations is related to the phase of the base state. The potential connection to a modal growth mechanism will be examined in future work.

References

1. Kleiser, L., Zang, T.A.. Numerical simulation of transition in wall-bounded shear flows. *Annual Review of Fluid Mechanics* 1991;**23**:495–537.
2. Suder, K.L., O'Brien, J.E., Reshotko, E.. Experimental study of bypass transition in a boundary layer. Tech. Mem. 100913; NASA; 1981.
3. Durbin, P.A., Wu, X.. Transition beneath vortical disturbances. *Annual Review of Fluid Mechanics* 2007;**39**:107–128.
4. Zaki, T.A.. From streaks to spots and on to turbulence: Exploring the dynamics of boundary layer transition. *Flow, Turbulence and Combustion* 2013;**91**:451–473.
5. Hunt, J.C.R., Carruthers, D.J.. Rapid distortion theory and the 'problems' of turbulence. *Journal of Fluid Mechanics* 1990;**212**:497–532.
6. Jacobs, R.G., Durbin, P.A.. Shear sheltering and the continuous spectrum of the Orr-Sommerfeld equation. *Physics of Fluids* 1998; **10**(8):2006–2011.
7. Zaki, T.A., Saha, S.. On shear sheltering and the structure of vortical modes in single- and two-fluid boundary layers. *Journal of Fluid Mechanics* 2009;**626**:111–147.
8. Klebanoff, P.S., Tidstrom, K.D., Sargent, L.M.. The three-dimensional nature of boundary layer instability. *Journal of Fluid Mechanics* 1962;**12**(01):1–34.
9. Landahl, M.T.. Wave breakdown and turbulence. *SIAM Journal on Applied Mathematics* 1975;**28**(4):735–756.
10. Landahl, M.T.. A note on an algebraic instability of inviscid parallel shear flows. *Journal of Fluid Mechanics* 1980;**98**:243–251.
11. Andersson, P., Brandt, L., Bottaro, A., Henningson, D.S.. On the breakdown of boundary layer streaks. *Journal of Fluid Mechanics* 2001; **428**:29–60.
12. Vaughan, N.J., Zaki, T.A.. Stability of zero-pressure-gradient boundary layer distorted by unsteady Klebanoff streaks. *Journal of Fluid Mechanics* 2011;**681**:116–153.
13. Hack, M.J.P., Zaki, T.A.. Streak instabilities in boundary layers beneath free-stream turbulence. *Journal of Fluid Mechanics* 2014;**741**:280–315.
14. Nolan, K.P., Zaki, T.A.. Conditional sampling of transitional boundary layers in pressure gradients. *Journal of Fluid Mechanics* 2013; **728**:306–339.

15. Bradshaw, P., Pontikos, N.S.. Measurements in the turbulent boundary layer on an 'infinite' swept wing. *Journal of Fluid Mechanics* 1985; **159**:105–130.
16. Driver, D.M., Hebbar, S.K.. Experimental study of a three-dimensional, shear-driven, turbulent boundary layer. *AIAA Journal* 1987; **25**(1):35–42.
17. Spalart, P.R.. Theoretical and numerical study of a three-dimensional turbulent boundary layer. *Journal of Fluid Mechanics* 1989;**205**:319–340.
18. Jung, W.J., Mangiavacchi, N., Akhavan, R.. Suppression of turbulence in wall-bounded flows by high-frequency spanwise oscillations. *Physics of Fluids A* 1992;**4**(8):1605–1607.
19. Quadrio, M., Ricco, P.. Critical assessment of turbulent drag reduction through spanwise wall oscillations. *Journal of Fluid Mechanics* 2004;**521**:251–271.
20. Kim, J., Moin, P.. Application of a fractional-step method to incompressible Navier-Stokes equations. *Journal of Computational Physics* 1985;**59**:308–323.
21. Rosenfeld, M., Kwak, D., Vinokur, M.. A fractional step solution method for the unsteady incompressible Navier-Stokes equations in generalized coordinate systems. *Journal of Computational Physics* 1991;**94**:102–137.
22. Jacobs, R.G., Durbin, P.A.. Simulations of bypass transition. *Journal of Fluid Mechanics* 2001;**428**:185–212.
23. Roach, P., Brierley, B.. The influence of a turbulent freestream on zero pressure gradient transitional boundary layer development, part I: Test cases T3A and T3B. In: *ERCOFTAC Workshop: Numerical Simulation of Unsteady Flows and Transition to Turbulence, Lausanne, Switzerland*. Cambridge University Press; 1990, p. 319–347.
24. Brandt, L., Schlatter, P., Henningson, D.S.. Transition in boundary layers subject to free-stream turbulence. *Journal of Fluid Mechanics* 2004;**517**:167–198.
25. Schrader, L.U., Brandt, L., Zaki, T.A.. Receptivity, instability and breakdown of Görtler flow. *Journal of Fluid Mechanics* 2011;**682**:362–396.
26. Baron, A., Quadrio, M.. Turbulent drag reduction by spanwise wall oscillations. *Applied Scientific Research* 1996;**55**:311–326.